Military Technical College
Kobry El-Kobbah,
Cairo, Egypt

7th International Conference
on Electrical Engineering
ICEENG 2010

Control of BLDC Motor for Satellite Momentum Exchange

Ibrahim M. Safwat*, Amgad S. Elwakeel*, Abd Elfattah Eliwa*, Prof. Dr. A. Abd Elsattar**

Abstract:

The reaction wheel is a small fraction of the spacecraft total mass. It permits very precise changes in spacecraft attitude. A novel model of a single-axis position control on a satellite is designed using Brushless DC (BLDC) motor with a resolver to exchange the momentum of the satellite as a reaction wheel. The technique of attitude control is based on considering the moment of inertia of the satellite as a part of the moment of inertia of BLDC motor, so the control on a satellite becomes the control of a Brushless DC motor. Two kinds of controllers are used (PID) controller and (FLC). The performance of both controllers is evaluated to explain the main characteristics of each one.

Keywords:
Attitude control of satellite, Mathematical model of Brushless DC Motor (BLDC), Proportional Integrator Differentiative (PID) controller, Fuzzy Logic Controller (FLC).

* Egyptian Armed Force
** Ain Shams University

1. Introduction:

During the past several years, there was a great concern of the modern electrical control system researchers towards the permanent magnet synchronous motors. The performance of these motors resembles the characteristics of a separately excited dc motor. These BLDC motors not only avoid many problems, which have been presented due to brushes such as the electrical sparking and wearing, but also due to their numerous advantages such as controllability, light weight and high efficiency, they emerged as one type of the modern electrical motors used in many industrial applications, especially in the medical and aero- space fields [1, 2].

In this paper, the data of one practical industrial motor has been selected, and then the operating characteristics of this motor were modeled, simulated and investigated.

One of the main contributions of this work is using resolver in attitude control of satellite instead of using gyroscopes. The results have a satisfactory performance with the motor understudy and attitude control response on the satellite.

2. Attitude control of satellite

The attitude control of the satellite is considered as a position control of the satellite about its axes to keep it in adequate position. In this work, three-axis stabilizations are employed, so the general equations of motion of satellite with reaction wheels are [3]

$$\begin{aligned} I_x\dot{\omega}_x + (I_z - I_y)\omega_z\omega_y &= (T_d)_x + (T_w)_x \\ I_y\dot{\omega}_y + (I_x - I_z)\omega_x\omega_z &= (T_d)_y + (T_w)_y \\ I_z\dot{\omega}_z + (I_y - I_x)\omega_y\omega_x &= (T_d)_z + (T_w)_z \end{aligned} \qquad (1)$$

Where I_x, I_y, I_z are the moments of inertia of a satellite in *x, y, z* axes, $\dot{\omega}_x, \dot{\omega}_y, \dot{\omega}_z$ are the angular accelerations of a satellite in *x, y, z* axes, $\omega_x, \omega_y, \omega_z$ are the angular speeds of a satellite in *x, y, z* axes, T_d is the disturbance torque and T_w is the reaction wheel torque.

For single axis control, the equation of motion of the satellite becomes [4]

$$I\ddot{\theta}_{sat} = -\dot{H} = -J\dot{\omega}_r \qquad (2)$$

Where $\ddot{\theta}_{sat}$ is the second differentiation of the satellite deviation angle, H is the momentum of the reaction wheel, J is the moment of inertia of the reaction wheel, ω_r is the angular speed of the reaction wheel, and I is the moment of inertia of the satellite.

The location of the reaction wheels in pitch, roll and yaw axes is illustrated as shown in Fig (1).

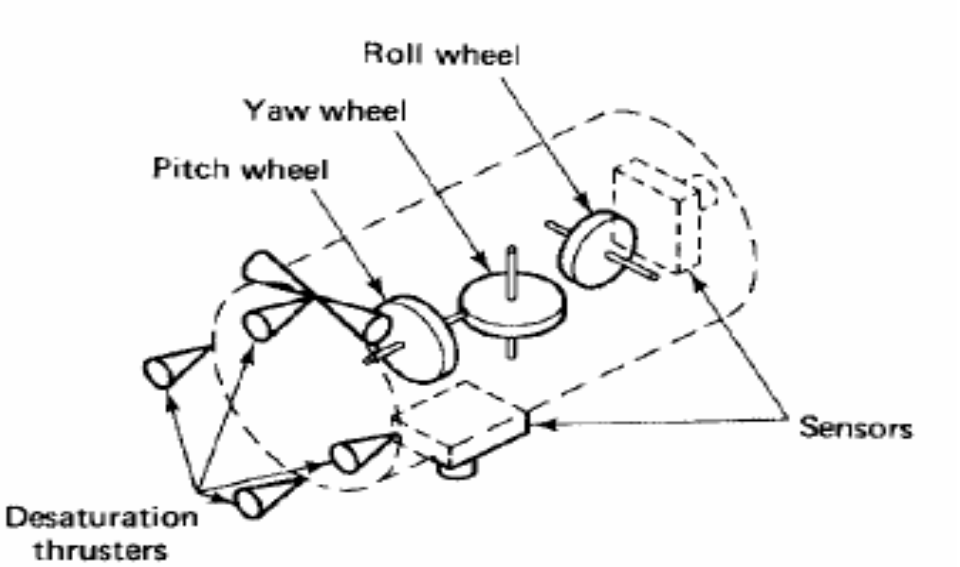

Figure (1): *location of reaction wheel in spacecraft*

So the single axis control of the satellite can be illustrated in the following block diagram.

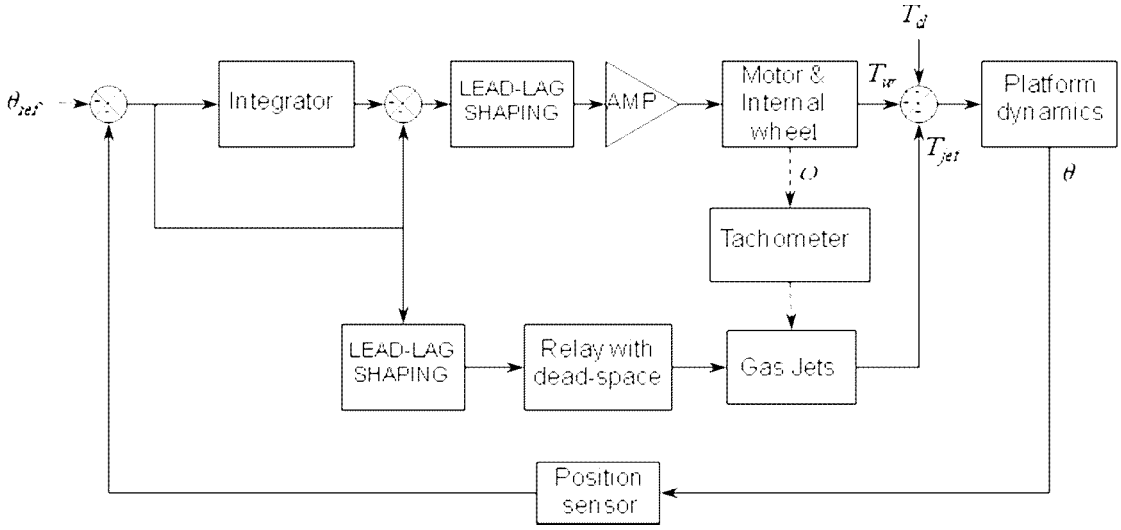

Figure (2): *Block diagram of single axis control of satellite*

The repointing control of the satellite from the initial direction to reach the target direction is illustrated in Fig (3). Because of the deviation due to the disturbance torque, the satellite needs to make a torque countering the disturbance torque.

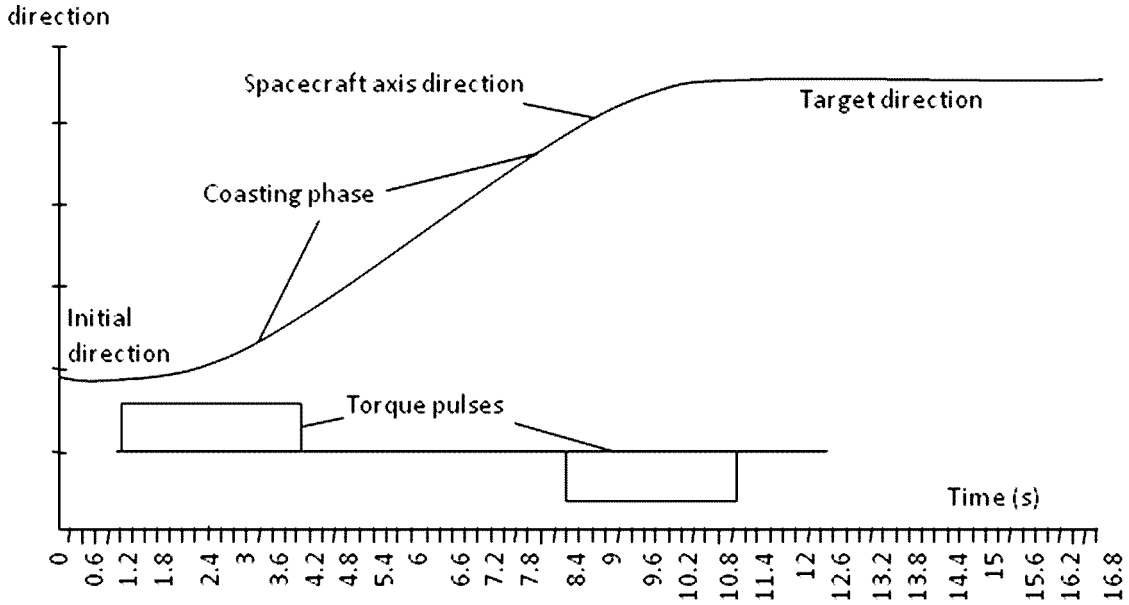

Figure (3): *Repointing about principle axis in three axis stabilization*

3. System model

3.1 Mathematical model of BLDC motor:

The state space representation of the BLDC motor is [3]:

$$\frac{d}{dt}\begin{bmatrix} i_a \\ i_b \\ i_c \end{bmatrix} = \begin{bmatrix} 1/(L-M) & 0 & 0 \\ 0 & 1/(L-M) & 0 \\ 0 & 0 & 1/(L-M) \end{bmatrix} \begin{bmatrix} v_a \\ v_b \\ v_c \end{bmatrix} - \begin{bmatrix} R & 0 & 0 \\ 0 & R & 0 \\ 0 & 0 & R \end{bmatrix} \begin{bmatrix} i_a \\ i_b \\ i_c \end{bmatrix} - \begin{bmatrix} e_a \\ e_b \\ e_c \end{bmatrix} \quad (3)$$

and $T_e = (e_a\, i_a + e_b\, i_b + e_c\, i_c)/\omega_r$ (4)

Where L, and R are the inductance and resistance of of each phase winding, i_a, i_b, i_c are the three-phase line currents, e_a, e_b, e_c are the three-phase EMFs and v_a, v_b, v_c are the input phase voltages to BLDC motor, T_e is the developed torque.

The equation of motion is:

$$\left(\frac{2}{p}\right)\frac{d\omega_r}{dt} = \frac{T_e - T_L - \left(\frac{2}{p}\right)B\omega_r}{J} \quad (5)$$

Where p is the number of poles, T_L is the load torque and B, J are the friction coeffecient and moment of inertia of the motor.

3.2 Resolver model

The resolver operates on the principle of a rotary transformer. In a rotary transformer the

rotor consists of a coil (winding) which, together with the stator winding, constitutes a transformer. The resolver is basically designed exactly in the same way, with the difference that the stator is made up of two windings displaced by 90° to one another, instead of one winding as shown in Fig (4). The resolver is used to determine the absolute position of the motor shaft over one revolution, especially with servo-drives. Furthermore, the speed and the simulation for the position control can be derived from the resolver signal [5].

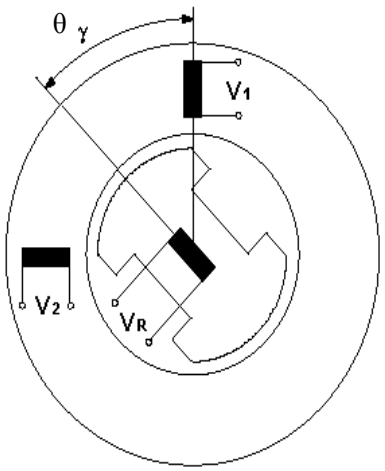

***Figure (4)**: Schematic design of the resolver*

The rotor of the resolver is mounted on the motor shaft as shown in Fig (5). Both the stator and the rotor are provided with an additional winding each to allow for brushless transmission of the stator primary voltage to the rotor. With the aid of these additional windings the primary voltage of the stator winding with a carrier frequency of 2-10 kHz is transmitted to the rotor (rotating transformer). The two windings carried on the rotor are coupled electrically so that the voltage transmitted from the stator to the rotor is also present on the second winding of the rotor.

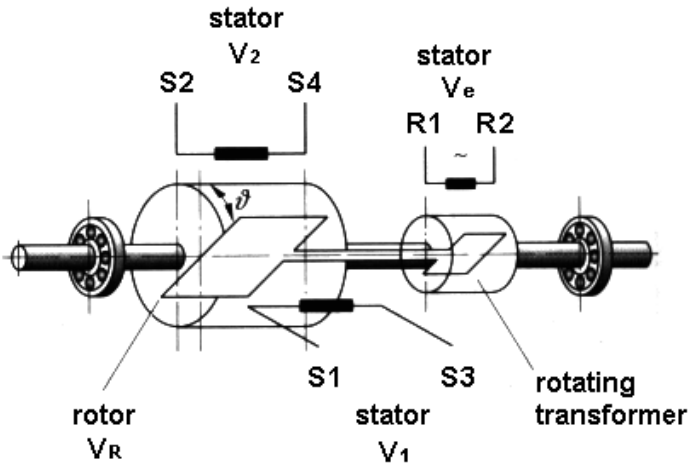

***Figure (5)**: the position of the resolver in the motor*

Voltages of different magnitudes are induced in the stator windings, depending on the position of the rotor. The winding through which there is full current flow at $\vartheta = 0°$ has the maximum voltage present at this point in time. If the rotor is rotating, then voltage V_1 on this winding decreases until it has attained the zero value at an angle of 90°. If the rotor is further rotated, the voltage again increases with inverse polarity until it has again reached its maximum at 180°. The voltage V_1 has a cosine curve as envelope. The voltage V_2, which is displaced by 90° from voltage V_1, has a value of 0 V at 0°. It increases until it has attained its maximum value at 90°, and then decreases again. The envelope of V_2 is therefore a sine curve. This is the known principle of amplitude modulation and it is illustrated in Fig (6).

The output voltages V_1 and V_2 are calculated as a function of the input voltage V_e by:

input: $V_e = V_s \sin(\omega t)$

output: $V_1 = V_s \sin(\omega t)\cos(\theta)$ (6)

$V_2 = V_s \sin(\omega t)\sin(\theta)$

Where θ is the rotor angle, ω is the carrier frequency of V_e, and V_s is the input voltage peak value.

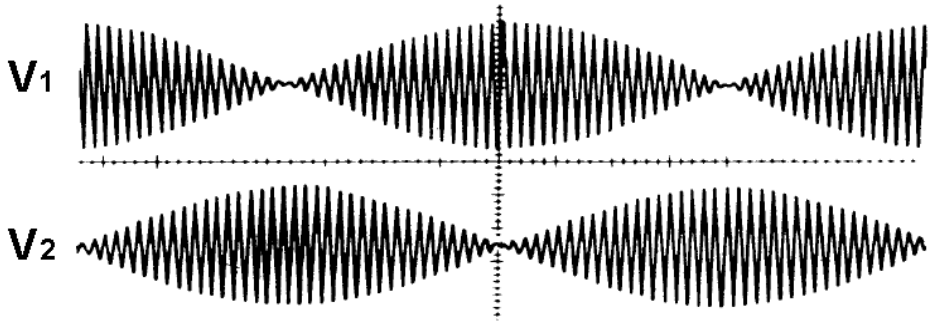

***Figure (6)**: output voltages V_1 and V_2 of the resolver*

4. Control philosophy

The philosophy of the satellite control is depends on the reference angle which is fixed at a target direction so it does not need complex adaptive control techniques and it is usually enough to use a simple PID controllers [6, 7].

4.1PID controller

This controller is a conventional type of control but if its parameters are adjusted precisely, it gives excellent results. The equation which represents the controller is

(7)

Where u(t) is the output of the controller, k_p is the proportional gain, k_i is the integral gain, and k_d is the differential gain.

In this paper, the optimization response toolbox of MATLAB is used to obtain the gains of PID controller. The general effects of control parameters are as shown in table (1).

Table (1): *Effects of parameters*[8]

Parameter	Rise Time	Time Overshoot	Settling Time	S.S. Error
Kp	Decrease	Increase	Small Change	Decrease
Ki	Decrease	Increase	Increase	Eliminate
Kd	Small Change	Decrease	Decrease	Small Change

4.2 Fuzzy Logic Controller

The input variables to the fuzzy logic controller were taken as the error of the angle (e) and the change in error (Δe) which are normalized by certain gain factors estimated by experience with some trials and error. These input variables have significant effects on the damping of shaft mechanical oscillations.

The membership functions for the linguistic variables are represented by symmetrical triangular shape causing precision control near the steady state operating point. The method used for defuzzification is the commonly used centroid method [9].

In this paper, the FLC generates reference voltage change (Δu) directly based on the position error e and its change Δe . These control input variables can be defined as:

$$\begin{aligned} e(k) &= \theta_r - \theta(k) \\ \Delta e(k) &= e(k) - e(k-1) \end{aligned} \tag{8}$$

where θ_r is the reference postion, $\theta(k)$ is the rotor postion at the current interval k , $e(k)$ is the position error and $\Delta e(k)$ is the change of error.

The output of the controller is the control voltage which is defined as:

$$U(k) = U(k-1) + k\,\Delta u \qquad (9)$$

where $U(k)$ is the fuzzy controller output, k is the fuzzy controller output gain and Δu is the inferred control output from the fuzzy controller.

Table (2) summarises the effects of fuzzy parameters. By applying the previous strategies, the fuzzy control gains k_e, k_{ce} and k have been estimated precisely.

Table (2): *Rule base fuzzy logic controller*

e / Δe	NB	NM	NS	ZE	PS	PM	PB
NB	NVB	NVB	NVB	NB	NM	NS	ZE
NM	NVB	NVB	NB	NM	NS	ZE	PS
NS	NVB	NB	NM	NS	ZE	PS	PM
ZE	NB	NM	NS	ZE	PS	PM	PB
PS	NM	NS	ZE	PS	PM	PB	PVB
PM	NS	ZE	PS	PM	PB	PVB	PVB
PB	ZE	PS	PM	PB	PVB	PVB	PVB

NV	Very Negative
N	Negative
P	Positive
S	Small
M	Medium
B	Big
BV	Very Big

Table (3)*: Effects of the fuzzy parameters k_e ,k_{ce}, and k* [9]

Gains		rise time	ringing	damping
k_e	⇑	decrease (**m**)	increase (**m**)	decrease (**m**)
	⇓	increase (**m**)	Decrease (**m**)	increase (**m**)
k_{ce}	⇑	increase (**w**)	increase (**s**)	increase (**s**)
	⇓	decrease (**w**)	decrease (**s**)	decrease (**s**)
k	⇑	decrease (**s**)	increase (**m**)	decrease (**w**)
	⇓	increase (**s**)	decrease (**m**)	increase (**w**)

s	strong effect
m	moderate effect
w	weak effect

Figs (7, 8) illustrate the membership function of the inputs (e, Δe) and the membership of the output.

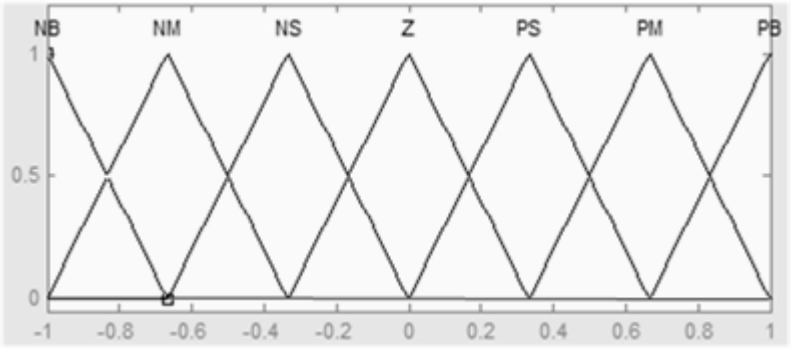

Figure (7): *The membership function of the inputs (e, Δe)*

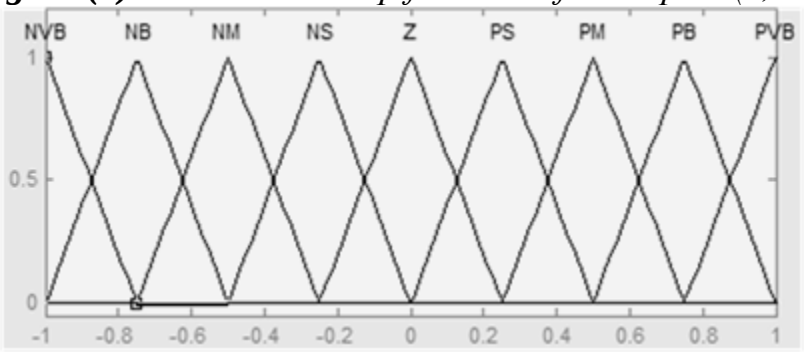

Figure (8): *The membership function of the output*

5. Simulation results

The specifications of the motor used in this work are:

Rated power = 0.5 kw, Rated speed = 6000 rpm, The nominal voltage = 190 V, Rated current = 3.4 A, Rated torque = 0.8 N.m.

The parameters used in the simulation are:

R=1.7 Ω, L=1.105 mH, J=0.45 kg.cm^2, λ=0.105 wb.

In this work, the moment of inertia of the spacecraft is added to the moment of inertia of the motor that means the spacecraft considered to be a part of the motor body. The worst case has been considered and it is about 180^o deviation from the target direction.

Fig (9) and Fig (10) describe the position control of BLDC motor using PID and Fuzzy controllers.

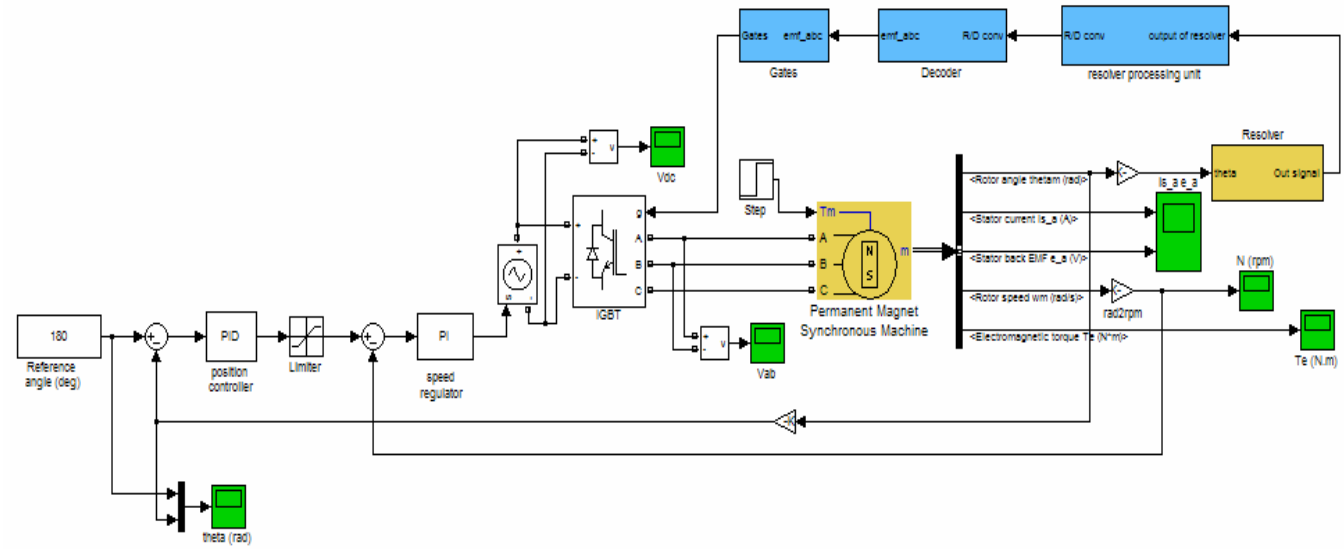

Figure (9): *Model of BLDC motor with PID controller*

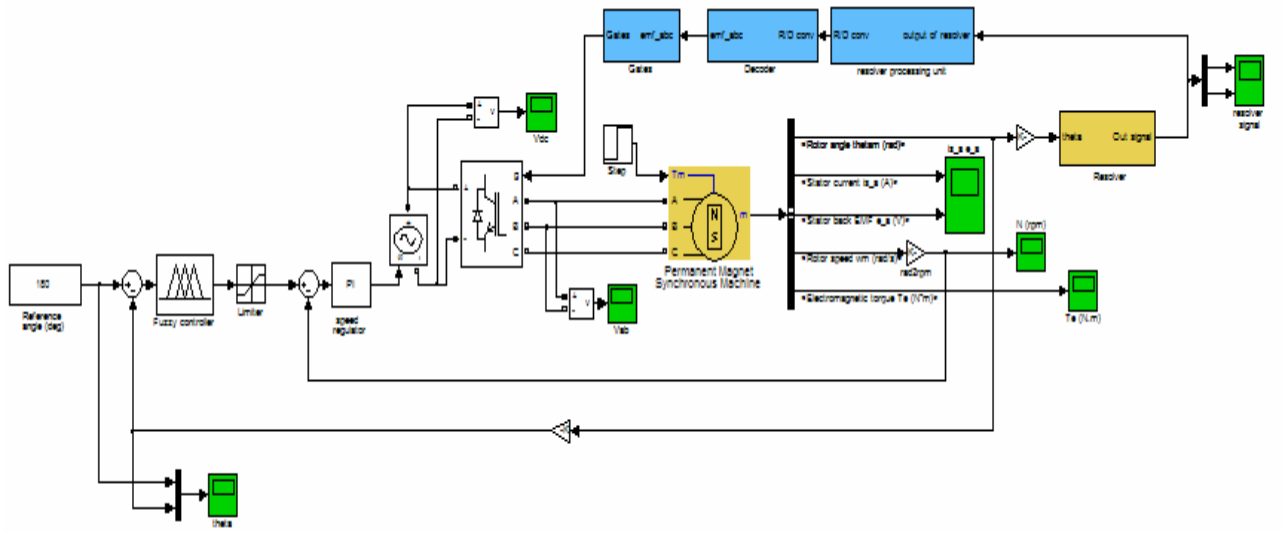

Figure (10): *Model of BLDC motor with Fuzzy logic controller*

6. The experimental setup

Fig (11) shows the block diagram of the closed loop system. In this implementation, real time application of LABVIEW is used to implement both PID and FUZZY controllers and the control unit of both PID and Fuzzy controllers as shown in Fig (10) and Fig (11).

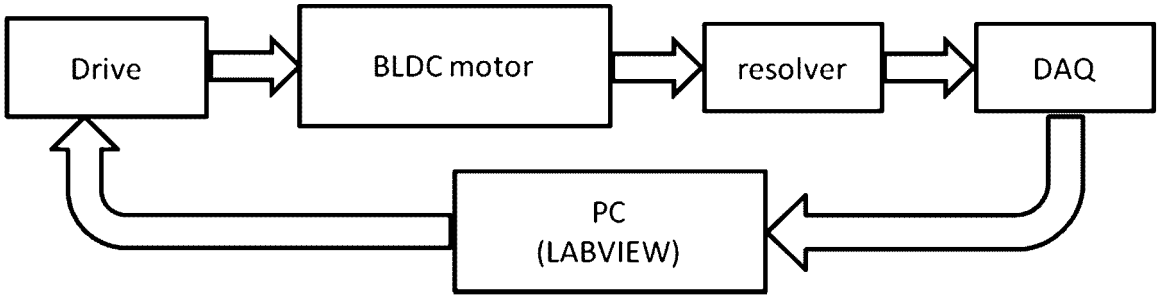

***Figure (11)**: Block diagram of the experimental work*

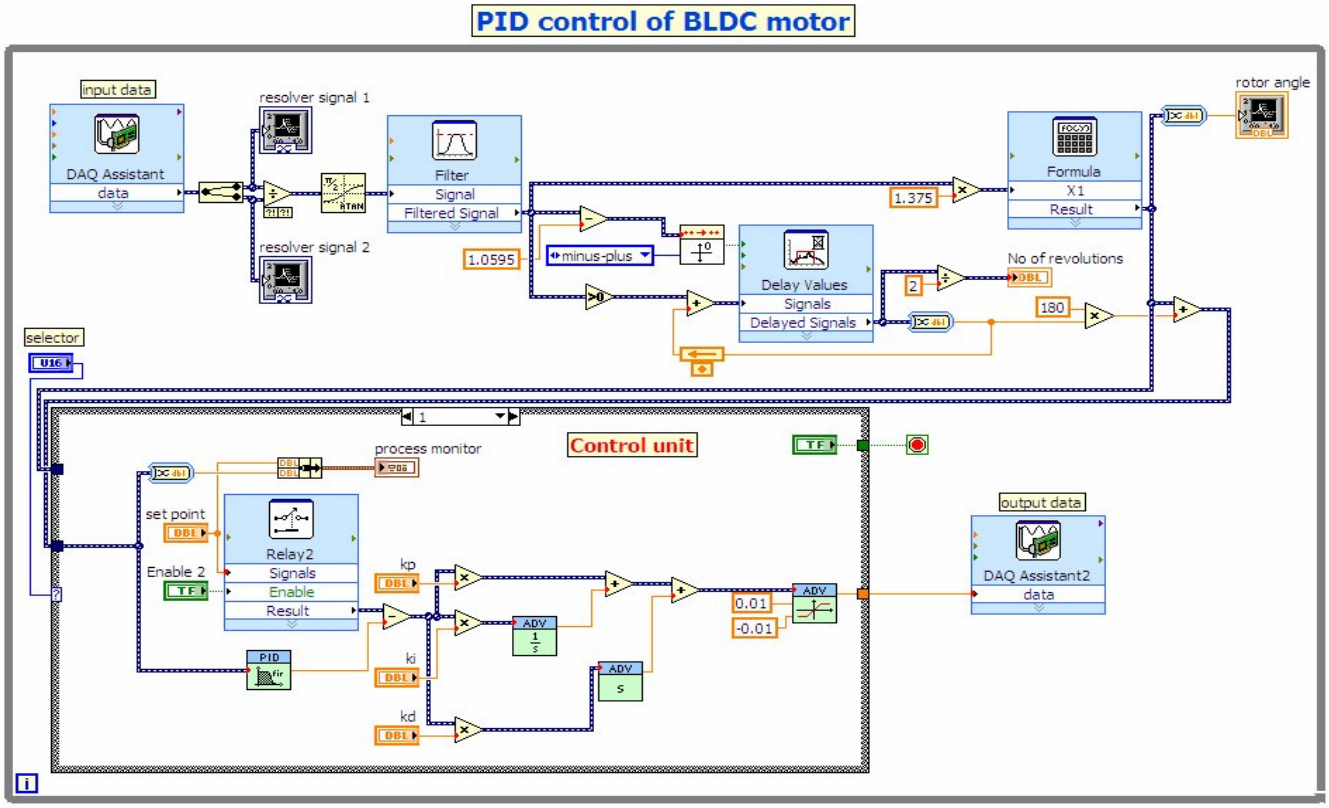

***Figure (12):** PID control of BLDC motor*

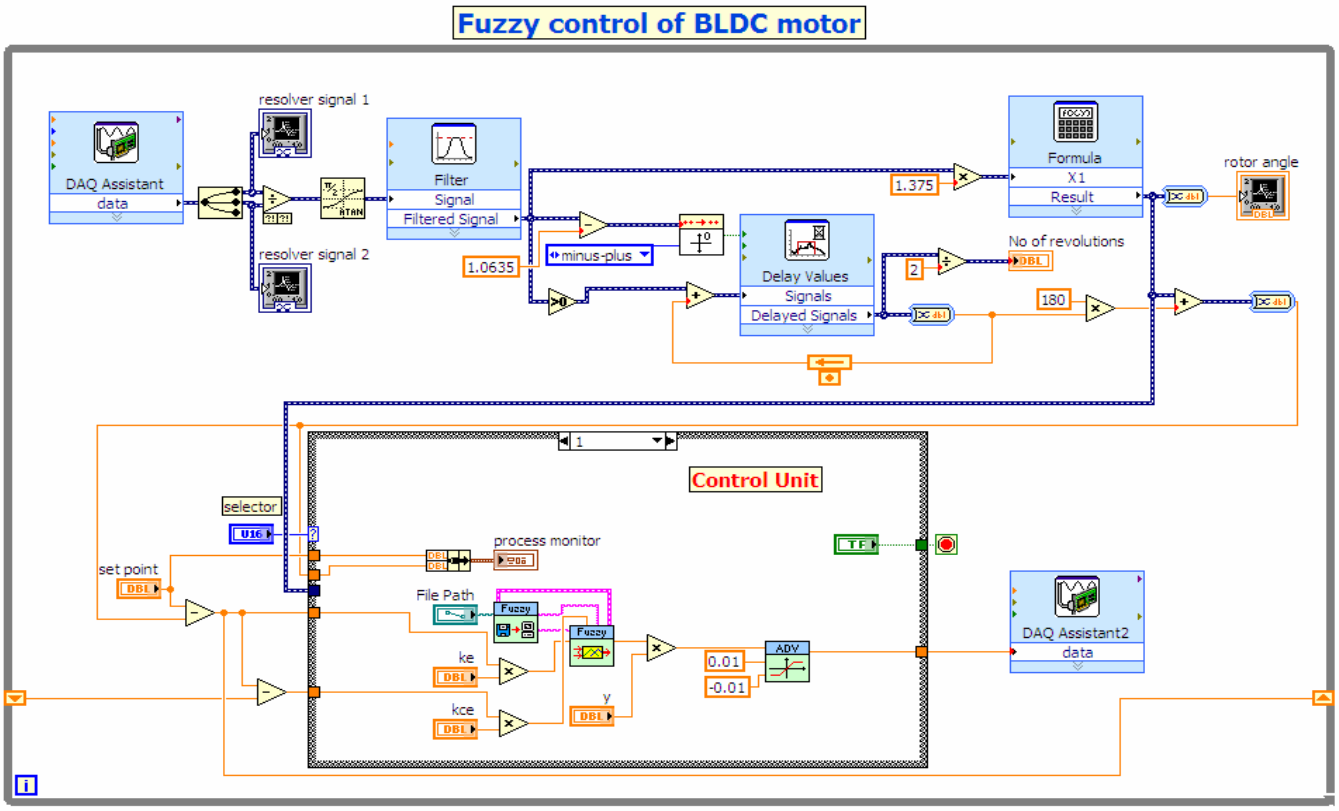

Figure (13): *FLC control of BLDC motor*

Fig (14) and Fig (16) show the output results of PID control and Fuzzy control in the experimental setup.

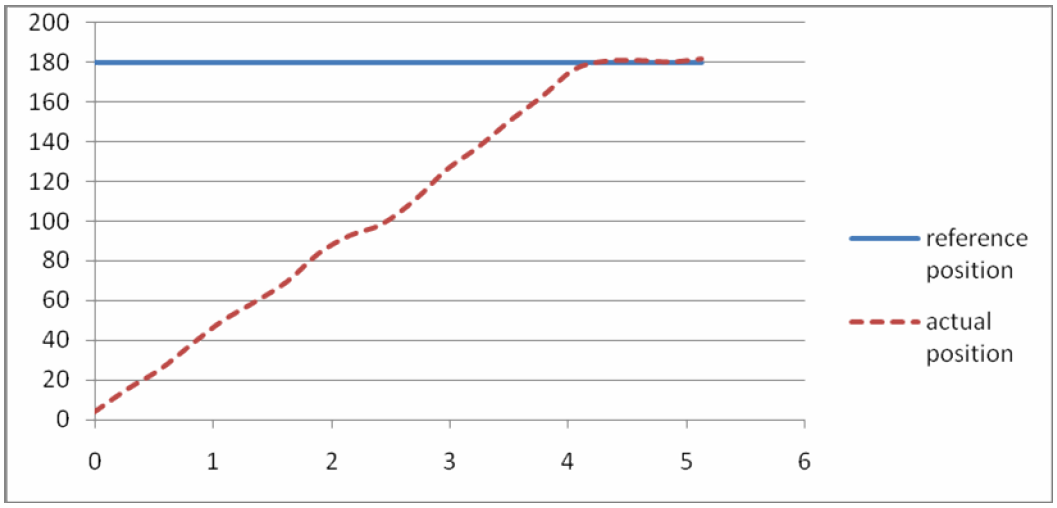

Figure (14): *Position control using PID controller in practical work*

The output results of PID control and Fuzzy control in the simulation are shown in Fig (15) and Fig (17).

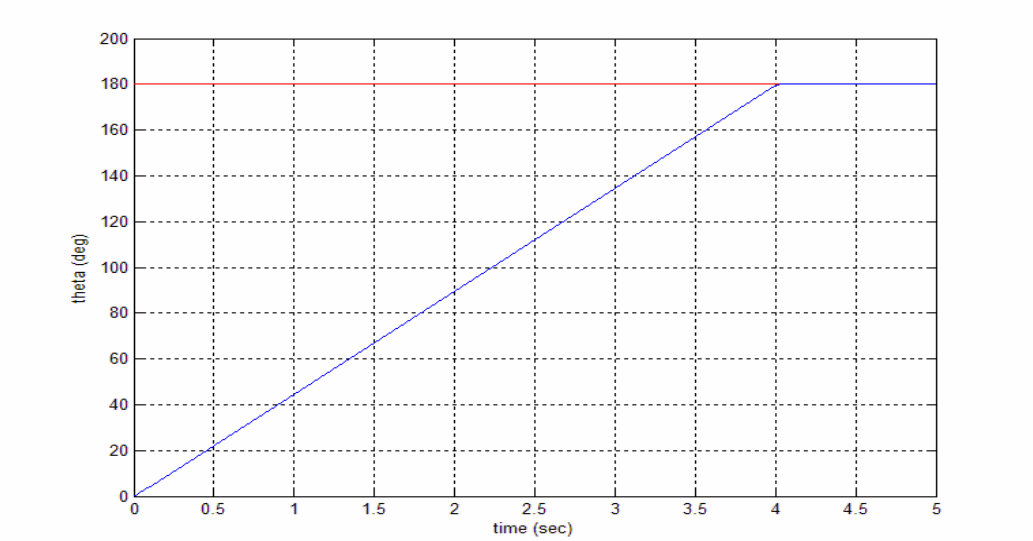

Figure (15): *Position control using PID controller in SIMULINK*

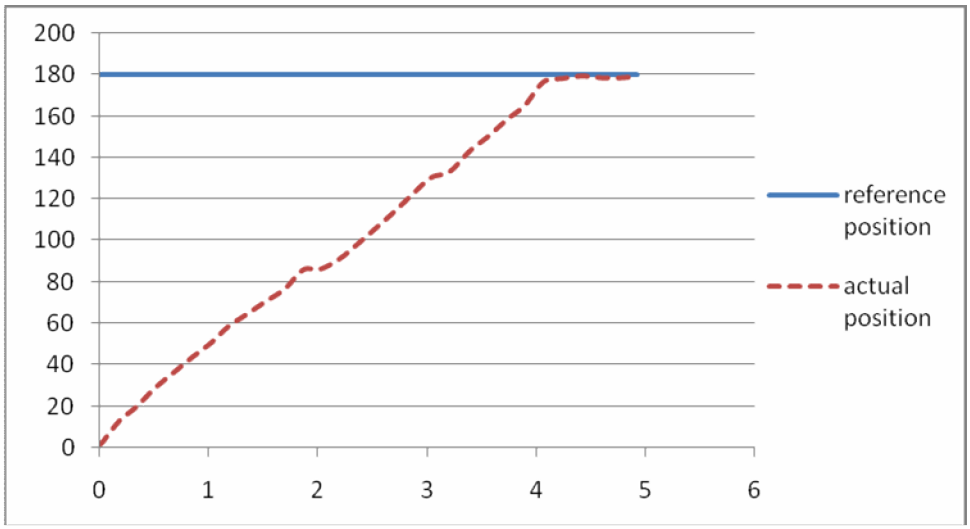

Figure (16)*: Position control using FLC in practical work*

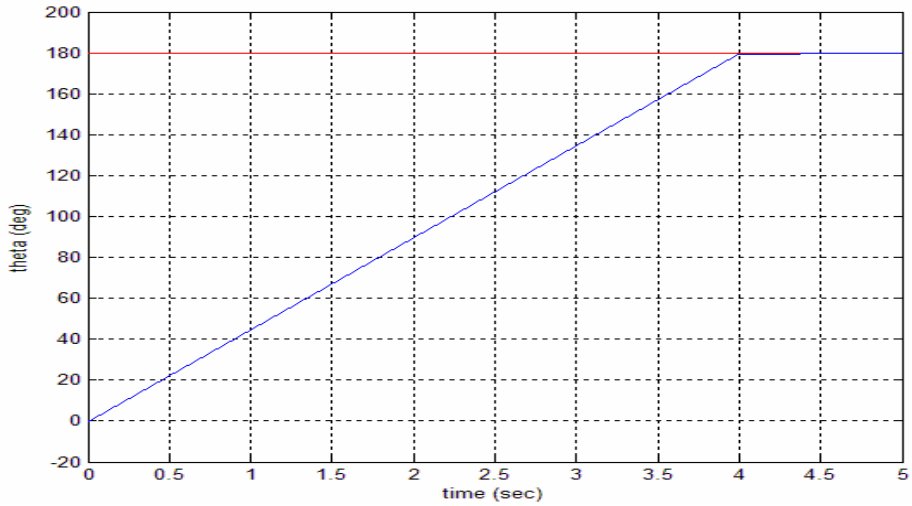

Figure (17)*: position control using FLC in SIMULINK*

Fig (18) shows that the rise time in PID control is less than in the FLC, there is no overshoot in both controls and a small steady state error is observed.

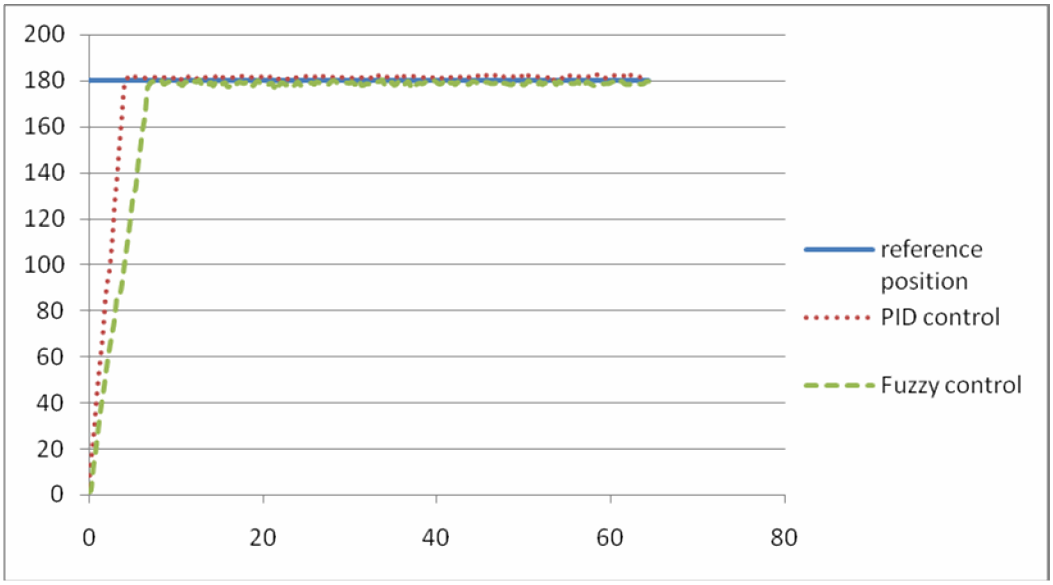

Figure (18): *comparison between PID control and FLC*

7. Conclusion:

An application of PID and FLC to BLDC motor for satellite position control has been presented. Both controllers are used to generate the change of reference voltage based on position error measured by a resolver.

The usage of a resolver as a position sensor gives very good accuracy about 0.1^{o} which gives precise changes in spacecraft attitude.

The comparison of the FLC and the PID controller demonstrate superior response with low rising time, no overshoot and negligible steady-state error.

References:

[1] M.A. Akcayol, Acetin, C Elmas" An Educational tool for fuzzy logic controlled BDCM" IEEE Transactions on Education, 2002.

[2] J.S. Lawler, JM.Baily, J.Pinto "Limitations of the Conventional Phase Advance Method for Constant Power Operation of the Brushless DC Motor ". IEEE Transaction on Power Electronics, 2004.

[3] J. S. Peter Fortescue, "spacecraft systems engineering," third ed: John Wiley and sons ltd, 2004.

[4] R. W. Froelid, "Reaction Wheel Attitude Control for Space Vechiles," *IRE National Automatic Control Conference,* 1959.

[5] P. Pillay, "Modeling of permanent magnet motor drives," *IEEE Transaction on industrial electronics,* vol. 35, november 1988.

[6] Nise, N. S. “Control systems engineering”, third ed., John Wiley & Sons, 2000.

[7] Schwarzenbach “Essential of control”, Longman, UK, 1996.
[8] S. o. U. Paderborn, "Rotational Measurements using a resolver," 2008.
[9] Astrom, "PID controllers- theory, design, and tuning," second ed, I. S. America, Ed., 1995.
[10] R. K. Mudiand, "A robust self tunning scheme for PI and PD type fuzzy controller," *IEEE Transactions on Fuzzy Systems,* vol. 7, 1999.
[11] M. N. Uddin, "performance of fuzzy ogic based indirect vector control for industry applications," 2002.